Geochemistry Geophysics Geosystems G3

Published by AGU and the Geochemical Society

Letter
Volume 14, Number 11
26 November 2013
doi: 10.1002/2013GC005001
ISSN: 1525-2027

Implications of a long-lived basal magma ocean in generating Earth's ancient magnetic field

L. B. Ziegler
College of Earth, Ocean, and Atmospheric Sciences, Oregon State University, 104 CEOAS Administration Building, Corvallis, Oregon, 97331-5503, USA (lbziegler@gmail.com)

D. R. Stegman
Ida and Cecil Green Institute of Geophysics and Planetary Physics, Scripps Institution of Oceanography, UC San Diego, La Jolla, California, USA

[1] Observations of Earth's magnetic field extending back to 3.45 billion years ago indicate that generation by a core dynamo must be sustained over most of Earth's history. However, recent estimates of thermal and electrical conductivity of liquid iron at core conditions from mineral physics experiments indicate that adiabatic heat flux is approximately 15 TW, nearly three times larger than previously thought, exacerbating difficulties for driving a core dynamo throughout Earth history by convective core cooling alone. Here, we explore the geomagnetic consequences of a basal magma ocean layer in the lowermost mantle, hypothesized to exist in the early Earth and perhaps surviving until well after the Archean. While the modern, solid lower mantle is an electromagnetic insulator, electrical conductivities of silicate melts are known to be higher, though as yet they are unconstrained for lowermost mantle conditions. We consider a range of possible electrical conductivities and find that for the highest electrical conductivities considered, a long-lived basal magma ocean could be a primary dynamo source region. This would suggest the proposed three magnetic eras observed in paleomagnetic data originate from distinct sources for dynamo generation: from 4.5 to 2.45 Ga within a basal magma ocean, from 2.25 to 0.4 Ga within a superadiabatically cooled liquid core, and from 0.4 Ga to present within a quasi-adiabatic core that includes a solidifying inner core.

Components: 6,241 words, 3 figures.

Keywords: paleomagnetism; Magma Ocean; thermal evolution of Earth.

Index Terms: 8125 Evolution of the Earth: Tectonophysics; 0325 Evolution of the atmosphere: Atmospheric Composition and Structure; 1595 Planetary magnetism: all frequencies and wavelengths: Geomagnetism and Paleomagnetism.

Received 19 August 2012; **Revised** 17 October 2012; **Accepted** 17 October 2013; **Published** 26 November 2013.

Ziegler, L. B., and D. R. Stegman (2013), Implications of a long-lived basal magma ocean in generating Earth's ancient magnetic field, *Geochem. Geophys. Geosyst.*, *14*, 4735–4742, doi:10.1002/2013GC005001.

1. Introduction

[2] Earth's initial thermal state is likely to be entirely molten as events such as the putative Moon forming impact and subsequent core formation generate sufficient heat to completely melt the mantle [*Stevenson*, 2007]. A terrestrial magma ocean that is global in scale can potentially evolve in a dramatically different fashion than those of other terrestrial bodies such as the Moon or Mars because of the much greater pressures reached in the lower mantle. Material properties of silicate

melts at lower mantle conditions are uncertain, but there is some indication that the mantle liquidus becomes steeper than liquid isentropes [*Mosenfelder et al*., 2007; *Stixrude et al*., 2009]. In this scenario, crystallization initiates at midmantle depths and proceeds down toward the core, resulting in isolation of a basal magma ocean (BMO) that is stably stratified with respect to the overlying solid mantle and may persist for billions of years [*Labrosse et al*., 2007].

[3] The electromagnetic properties of a magma ocean at lower mantle pressure and temperature conditions have not been directly constrained. The electrical conductivity of the solid lower mantle is estimated to be of order 10^0-10^1 Sm^{-1} [*Katsura*, 2007; *Velimsky*, 2010]. It is an insulator with respect to the strongly conducting core beneath, but is a stronger conductor than the crust and upper mantle. Higher values of conductivity (ca. 10^2 Sm^{-1}) have been inferred in the lowermost mantle, either in patches [*Nagao et al*., 2003] or bulk [*Constable and Constable*, 2004], possibly related to iron enrichment [*Otsuka and Karato*, 2012] or high-pressure postperovskite [*Ohta et al*., 2008]. Conductivity of silicates increases significantly upon melting due to increased ionic conduction [*Katsura*, 2007].

[4] Additionally, at sufficient pressure and temperature conditions (i.e., lower mantle and beyond), liquid oxides become weakly metallic with associated increases in electrical conductivity between 2 and 3 orders of magnitude [*Knittle and Jeanloz*, 1986; *Hicks et al*., 2006; *Spaulding et al*., 2012; *McWilliams et al*., 2012]. The presence of highly mobile ions such as H^+, K^+, and Na^+, common in hydrated and carbonated melts, are also expected BMO components that would be sequestered within the BMO upon its formation. These volatiles reduce melting temperatures and are expected to enhance electrical conductivity, as has been advocated for melts in the upper mantle [*Karato*, 1990; *Gaillard et al*., 2008; *Ni et al*., 2011].

[5] Here we explore the geomagnetic implications of a proposed basal magma ocean and comment on the limited paleomagnetic observations available in the Archean in relation to our results. We quantify expected convective velocities in the BMO region approximating the driving forces as thermal only. Based on extrapolations from the literature discussed above, we consider a range of electrical conductivity for BMO liquids between 10^2-10^4 Sm^{-1}, and discuss the role of this layer in geodynamo generation.

2. Methods

2.1. Dynamo Criteria and Magnetic Reynolds Number

[6] A self-sustaining planetary magnetic field can be generated through dynamo action in a vigorously convecting, electrically conductive fluid planetary layer under qualifying conditions. The exact bounds on conditions necessary for planetary dynamos are unknown, but certain criteria have been described for a thermally driven dynamo [*Stevenson*, 2003] and serve as a useful starting point for exploring whether the dynamic regime of the BMO may plausibly support dynamo action.

[7] The flow must be sufficiently three-dimensionally complex, with a radial component in the flow, as in the case of convection. Significant influence from the Coriolis force in a rotating fluid leads to helictical and cyclonic fluid motions, which have been shown to be favorable for dynamo generation. In terms of the Rossby number, a rough criterion [*Stevenson*, 2003] is that $Ro = v/2\Omega L < 1$, where Ω is the planetary rotation rate. Rotation rate of the early Earth was faster than today, with 6 h days following the moon forming impact [*Cuk and Stewart*, 2012]. Taking this rotation rate, a typical velocity of 1 cm/s, and a length scale of 800 km, a corresponding Rossby number is ca. 10^{-5}, which is $<<1$ indicating rotationally dominated fluid motions in a BMO region, conducive to dynamo generation.

[8] Additionally, the magnetic Reynolds number (a ratio of overturn to magnetic diffusion times) must exceed a critical value of about 10–100 for dynamo action [*Stevenson*, 2003], and is typically calculated as $R_m = vL\mu_o\sigma$, where μ_o is the permeability of free space, σ is electrical conductivity, v is the characteristic fluid velocity, and L is the length scale of fluid flow.

[9] In the scenario of a vigorously convecting BMO layer overlying an electrically conductive core, the core is not completely passive in magnetic field generation. The BMO is expected to suppress core convection (see section 3 and *Labrosse et al*. [2007]), leaving a stably stratified core consisting of negligible radial fluid motions. However, the core is likely to contain strong horizontal flows and shear, resulting from any of a number of causes such as differential rotation, tidal forcing, and precession, and these will be very effective at producing strong toroidal fields from any poloidal field generated in the BMO layer. In such a scenario, it is the product of

magnetic Reynolds numbers of the two regions that must be sufficiently large for dynamo action, not just that in the BMO layer. This is the case in the Sun, where toroidal field is generated in the Tachocline below the convective layer [*Parker*, 1979]. In the case of the BMO dynamo, the core's toroidal field would be reduced by the lower conductivity in the BMO but would still reinforce the regeneration of poloidal flux. The critical magnetic Reynolds number in the BMO alone could therefore be substantially below the normal threshold for dynamo action. The product of the magnetic Reynolds numbers is denoted as the Dynamo number, D, where $D=(R_{m\_core})^{1/2}(R_{m\_bmo})^{1/2}$, and we adopt a value of 100 as our nominal critical value for dynamo action.

[10] R_{m_core} is held constant during the BMO era, and calculated with the approximation that velocity is of the order of modern core surface velocities. Using $v_{core}=5x10^{-4}$m/s [*Holme*, 2007], $\sigma_{core}=1.5x10^{6}$S/m [*Pozzo et al.*, 2012], and $L_{core}=3.5x10^{6}$m, we have $R_{m\_core}=3500$ and $R^{1/2}_{m\_core}=60$. We focus on investigating the temporal evolution of D dependent on the time-varying R_{m_bmo}. For this, the length scale is taken to be the BMO thickness, which decreases with time. In the case of thermally driven convection, velocities are related to heat flux through the layer. We therefore model and calculate heat flux through the BMO, from there estimate velocities through appropriate scaling laws, and then estimate R_{m_bmo} using a range of electrical conductivities.

2.2. Thermal History

[11] Earth's heat loss over time is governed by solid-state mantle convection and although it depends on the amount of long-lived radiogenic heat production, the strong dependence of mantle viscosity on temperature allows for self regulation [*Davies*, 1980]. Inferences of mantle temperature through time based on petrologic studies [*Abbott et al.*, 1994; *Herzberg et al.*, 2010] suggest cooling rates of $\sim$150−300° K since 3 Ga. Backward time integration of thermal history models based on boundary layer theory that relate the evolving temperature in Earth's interior to the surface heat flow starting at present-day values lead to mantle temperatures that exceed the mantle solidus by 3 Ga (i.e., a thermal catastrophe) [*Davies*, 1980]. Such models are incompatible with inferred temperatures of the Archean [*Herzberg et al.*, 2010].

[12] This motivated alternative cooling models that empirically fit constraints on the Earth's heat loss, for example, parameterizations that assume constant heat flow over time [*Labrosse and Jaupart*, 2007]. Such a model was consequently applied to investigate the scenario of a crystallizing BMO [*Labrosse et al.*, 2007] (Figure 1a, dashed lines) in which heat production and latent heat within the BMO delay secular cooling of the mantle and core (Figure 1b, dashed lines).

[13] We model the thermal evolution using the methods of *Labrosse et al.* [2007], which solves for the thermal evolution by backward time integration of a set of two coupled partial differential equations. Radiogenic elements are approximated to be perfectly incompatible, with the BMO hosting a constant fraction (20%) of the bulk silicate Earth complement of radioactive elements through time. We modify three parameters to create our preferred model. Q_m, the present-day heat flow out of the BMO, is 19 TW (instead of 15 TW) which accounts for 15 TW of core cooling and the 4 TW of radiogenic heating. The present-day thickness of the liquid mantle layer, a_o, is 100 m instead of 5422 m. The enrichment of melt in dense components relative to the crystallizing solid, $\Delta\xi$, is changed from 0.088 to 0.05 which represents slightly more conservative estimates of iron fractionation occurring during the solidification of the BMO. These changes are all within the significant uncertainty. The resulting preferred model is presented in Figure 1a (evolution of the temperature and thickness of the BMO layer), and Figure 1b (evolution of heat fluxes) and discussed in section 3.

2.3. Characteristic Velocities

[14] Viscosity of a basal magma ocean is expected to be higher than that of the core by roughly a couple orders of magnitude (10^{-1} Pa s [*Solomatov*, 2007] for BMO versus 10^{-3} Pa s for the outer core [*Vocadlo*, 2007]). This would slightly reduce the influence of rotation on the flow as well as the amount of turbulence [*Solomatov*, 2007], suggesting that mixing length theory would be a reasonable place to start for estimating characteristic velocities in the BMO:

$$v_{ml} \sim (Q_m L\alpha g/\rho c_p)^{1/3} \quad (1)$$

where Q_m is the heat flow out of the BMO into the overlying solid mantle and is obtained from the thermal evolution model, L is the length scale taken to be the height of the BMO, α is the thermal expansivity, g is gravitational acceleration, ρ is the BMO density, and c_p is the specific heat.

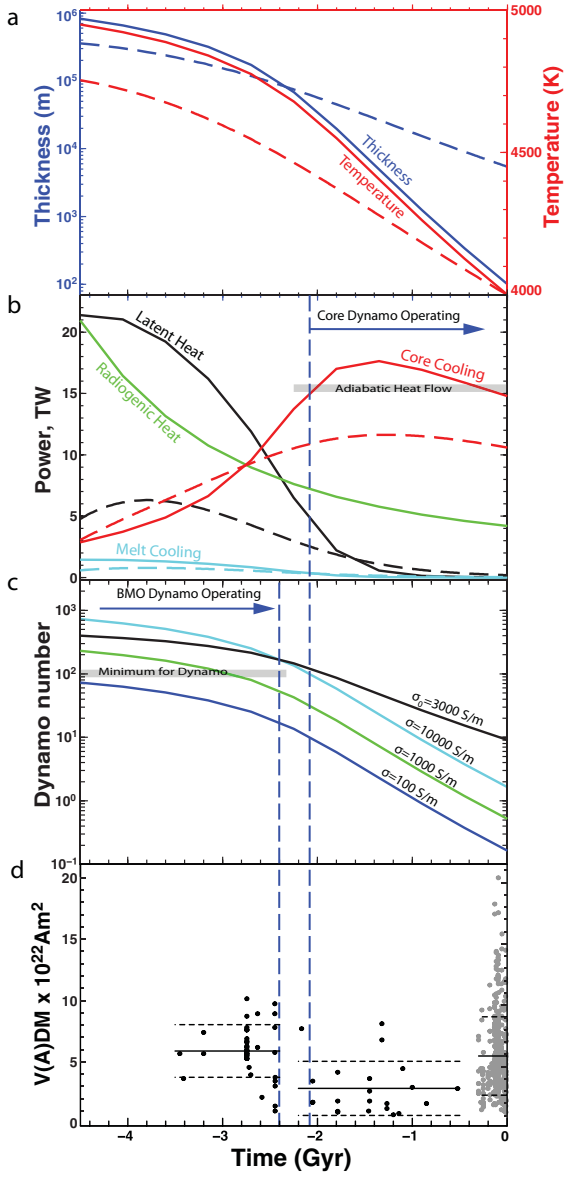

Figure 1. Thermal and geomagnetic evolution of Earth: (a) thickness and temperature of mantle "basal magma ocean" layer through time. Dashed lines represent previously hypothesized BMO [*Labrosse et al.*, 2007]. Solid lines represent updated model. (b) Heat budget—latent and radiogenic heat terms represent sources within the BMO. Melt cooling is mantle melt layer. Solid and dashed as in Figure 1a. Adiabatic heat flow [*Pozzo et al.*, 2012], which must be surpassed for thermally driven convection and dynamo in core indicated. (c) Dynamo number of BMO-core region using constant and time-varying electrical conductivities (labeled). Minimum D for dynamo action indicated. (d) Reproduced after *Biggin et al.* [2009]. Paleomagnetic field intensity data older than 0.5 Gyr ago (black) and 10–500 Gyr ago (gray) compiled in the PINT database [*Biggin et al.*, 2009] which pass reliability criteria [*Biggin et al.*, 2009]. Mean and one standard deviation of three proposed geomagnetic eras calculated and shown as solid and dashed lines, respectively. Dashed vertical lines highlight time window of transition between mantle and core dynamos which may have left the Earth temporarily without a magnetic field.

[15] We nonetheless also calculate velocities using scaling laws which include the influence of rotation, Ω. First, we include velocities estimated using scalings developed for the "hard turbulence" convective regime, applicable to cases of high Rayleigh numbers, such as a magma ocean, where large-scale circulation develops (see review in *Solomatov* [2007]):

$$v_{HT} \sim 14 * (Q_m \alpha g / \rho \Omega c_p)^{1/2} \quad (2)$$

[16] Also shown are two velocity scaling laws developed for the Earth's core:

$$v_{MAC} \sim (Q_m \alpha g / \rho \Omega c_p)^{1/2} \quad (3)$$

$$v_{CIA} \sim (Q_m \alpha g / \rho c_p)^{2/5} (L/\Omega)^{1/5} \quad (4)$$

where v_{MAC} results from a balance of buoyancy forces against the Lorentz force, which is taken to be of order of the Coriolis force [*Starchenko and Jones*, 2002] and v_{CIA} results from a balance of Coriolis, Inertia, and Buoyancy ("Archimedean") terms in a vorticity equation [*Aubert et al.*, 2001]. See review in *Christensen* [2010] for further details on their derivation.

3. Results

[17] The time evolution of D (Figure 1c) is found using v_{ml} for several values of σ, including a representative time-varying conductivity with a starting value of 3000 Sm^{-1} which increases with time (ca. 1 order of magnitude over the period 4.5–2.5 Ga) due to expected iron enrichment through fractionation as crystallization progresses and the mass of the BMO decreases. Velocities are not plotted directly but range between 0.8 and 1.4 cm/s obtained using mixing length theory. Adopting the minimum value of $D = 100$, a dynamo may operate until 2.5 Ga for $\sigma(t)$, $\sigma = 10000$ Sm^{-1}, and $\sigma = 1000$ Sm^{-1}. As R_{m_bmo} depends on the average length scale of convection (taken here as the thickness of the BMO), the decrease in R_{m_bmo}, and hence D, is largely attributable to solidification of the BMO. It is unclear whether a minimum layer thickness is required for dynamo generation irrespective of R_m.

[18] An initially ~800 km thick BMO provides a significant portion of the early Earth's energy budget. Radioactive and latent heat generation within the basal magma ocean suppress core heat flow, preventing thermally driven convection and magnetic field generation within the core

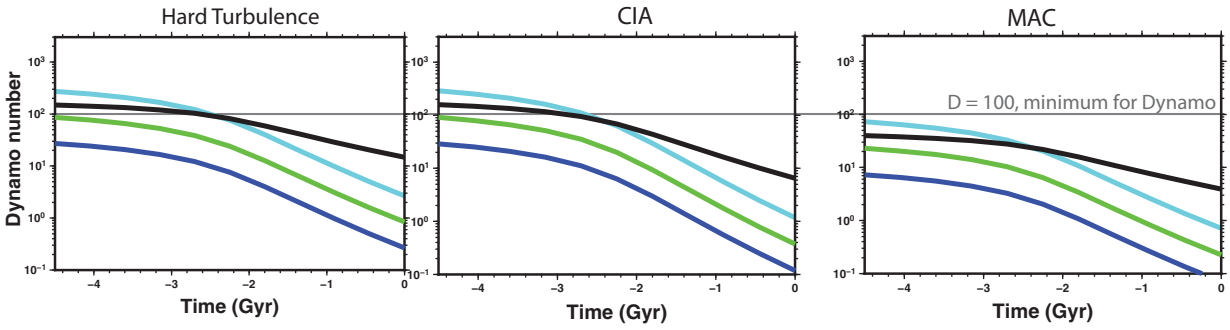

Figure 2. Dynamo number, D, calculated from thermal history model using several alternate velocity scaling laws: D when using velocity scaling from "hard turbulence" scaling law developed for (left) magma oceans, using (middle) CIA balance and (right) MAC balance developed for magnetic cores (see text). Theoretical minimum D marked as gray line. Colors as in Figure 1c.

[*Labrosse et al*., 2007]. Only after the BMO has significantly crystallized does core heat flow reach a maximum (Figure 1b). Delayed cooling of the core helps reconcile models of a young inner core of about 300–400 Ma [*Pozzo et al*., 2012]. In the originally proposed model of *Labrosse et al*. [2007], onset of the core dynamo began around 3.5 Gyr ago (dashed red line, Figure 1b) based on $Q_{ad} = 5$ TW, coinciding with the age of the oldest measured paleomagnetic field intensity [*Tarduno et al*., 2010]. However, revised estimates [*Pozzo et al*., 2012] put $Q_{ad} = 15$ TW and now suggest a soley thermal dynamo would never be achieved in their original BMO model. Core heat flow in our model is suppressed until 2.1 Ga, much later than the oldest observed paleomagnetic field. For the period pre-2.1 Ga, our model suggests the BMO could play a role in dynamo generation.

[19] Alternate velocity scalings give lower values for associated convective velocities, and correspondingly smaller values for Dynamo number. Figure 2 plots D using the three alternate scalings discussed in the methods section. For MAC balance velocities, D is lower than critical and if this is the most appropriate scaling, dynamo generation is unlikely even at the highest electrical conductivities used here. The CIA balance and hard turbulence regime scalings give intermediate results, where D is above critical for billions of years for the highest values of σ.

4. Paleomagnetic Observations of the Ancient Field

[20] The long term evolution of the Earth's magnetic field is preserved in the rock record through the magnetization of iron-bearing minerals crystallizing in the presence of the field. *Biggin et al*. [2009] classified paleomagnetic field intensity measurements between 10 Ma and 3.5 Ga into three distinct magnetic eras. In Figure 1d, we reproduce their result, using an updated version of PINT database (15 August 2012 date of last modification, http://earth.liv.ac.uk/pint/). Following their methods, the PINT database is first filtered to select data meeting reliability criteria outlined in *Biggin et al*. [2009]. The update includes approximately 150 additional data younger than 300 Ma, and five new references producing 29 data older than 500 Ma which meet the selection criteria. Samples younger than 300 Ma represent field strengths typical of the modern field (mean of 5.37 $\times$ 10^{22}Am^2) which are comparable to those from the Archean (mean of 6.01 $\times$ 10^{22}Am^2). The time span corresponding to the Proterozoic represents an era of lower field strength (mean of 3.01 $\times$ 10^{22}Am^2). Additional data are needed to resolve whether these initial estimates reflect robust differences in field characteristics and geodynamo behavior during the modern, Proterozoic, and Archean paleofields.

[21] The thermal history model presented here suggests a three stage evolution of magnetic field generation (Figure 3) starting with a thin-shell dynamo within the BMO until 2.5 Ga, followed by a core dynamo driven at first only by thermal convection during a period of superadiabatic core cooling and later with additional power sources arising from inner core solidification (i.e., the modern dynamo). A testable prediction of the BMO dynamo is the subsequent hiatus of magnetic field generation until $Q_{cmb} > Q_{ad}$, during which rocks will lack a detectable paleomagnetic

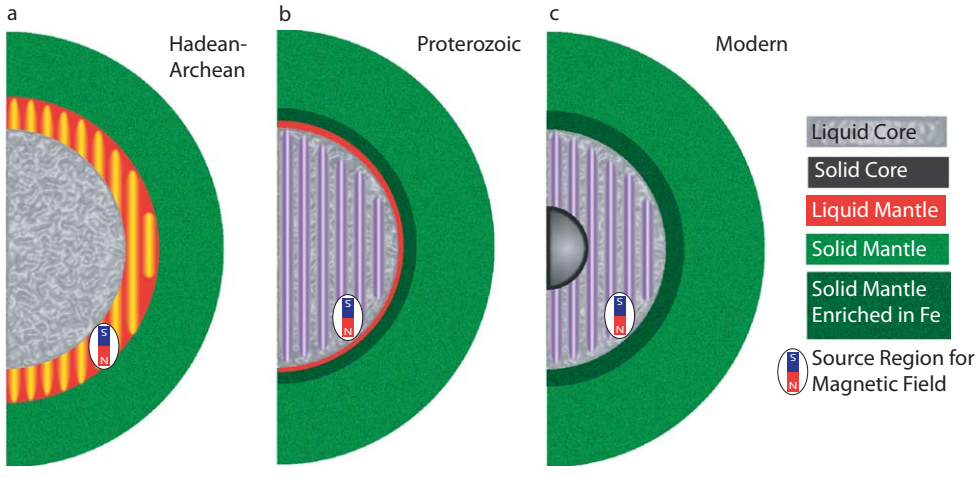

Figure 3. Illustration of three phases of geodynamo generation: (a) Earliest earth until circa 2.5 Ga, a basal magma ocean in the mantle hosts a thin-shell dynamo. Vertical columns represent rotationally dominant convective fluid motions. (b) Second stage, characterized by an almost fully solidified mantle, where last crystallization products are compositionally Fe enriched and dense. Greater heat flux out of core allows for thermal convection to drive dynamo in fluid core. (c) As core cools, solid inner core initiates and grows. Geodynamo powered by thermal and compositional convection enhanced by core solidification, leading to stronger average field strength.

signature. This magnetic hiatus occurs in the model around 2.4–2.15 Ga (Figure 1c) and seemingly corresponds to a gap in the collected data from 2.45 to 2.25 Ga (Figure 1d). In this scenario, observations from lunar samples which imply a lack of magnetic field on Earth at some point post-3.9 Ga [*Ozima et al*., 2005] can be reinterpreted as corresponding to this gap in magnetic shielding during the Archean era transition from mantle to core dynamos, and not prior to initiation of core dynamo between 3.9 and 3.5 Ga, as was interpreted previously [*Ozima et al*., 2005]. Though the true gap could be much shorter, and hard to resolve with the sparsity of Archean rocks suitable for paleomagnetic experiments, we encourage the reporting of "failed" paleointensity experiments, where there are no clear rock magnetic explanations for such results, which otherwise might not be published.

[22] The geometry of the magnetic field generated in the BMO would likely differ from the modern field. Thin-shell dynamos are less dipolar, where the specific structure of the nondipole field is dependent on the aspect ratio of the shell radius to the radius of the interior nonconvecting region (here, the core) [*Stanley and Bloxham*, 2006]. Paleomagnetic field directions indicate the Archean field was more antisymmetric [*Smirnov et al*., 2011] than the present-day field. A heavily antisymmetric field is consistent with numerical simulations of a very thin shell surrounding a stably stratified fluid core (aspect ratio of 0.8) where the resulting field was dominated by dipole and octupole terms [*Stanley and Bloxham*, 2006]. For reference, the aspect ratio for a 1000 km thick BMO over the fluid core is approximately 0.78. The higher strength of the Archean relative to the Proterozoic could represent insight about the magnetic energy available, or additionally could be a function of Earth's surface being closer to the dynamo source region when the BMO is hundreds of kilometers above the present-day core-mantle boundary (CMB).

5. Discussion

[23] This model demonstrates the feasibility of dynamo generation from thermal convection in a long-lived liquid mantle layer overlying a fluid iron core. Future work toward a more realistic portrait of a mantle dynamo should include effects of compositional convection inherent in the solidification process which will enhance convection and dynamo efficiency [*Buffett et al*., 1996]. In the modern core, concentration of light elements at the inner core boundary occurs as the inner core solidification process fractionates them into the liquid. This acts as an important source of buoyancy in the fluid outer core, driving convection

and dynamo action. A solidifying BMO represents a much more complex picture of starting and evolving composition (see e.g., C. Jackson et al., A geochemical evaluation of potential magma ocean dynamics using a parameterized model for perovskite crystallization, submitted to *Earth and Planetary Science Letters*, 2013). A greater understanding of the high-pressure/temperature phase diagram and partitioning behavior is needed for quantifying compositional stirring, but it is very likely to be an important factor.

[24] Figures 1 and 2 show several combinations of velocity and electrical conductivity conditions, which would be favorable for dynamo generation in the BMO. While we suggest that paleomagnetic data favor a 2 Gyr BMO dynamo duration, a range of longevities are possible given the weak constrains available. Also, as shown, there are cases where the combination of fluid velocities and electrical conductivity of the BMO layer would fall short of being sufficient for dynamo generation, as per the Dynamo number criteria. In such cases the BMO may still have a more indirect role in amplifying or dampening a nonthermal core dynamo or affecting the field geometry.

6. Conclusions

[25] The model of *Labrosse et al*. [2007] presents an ancient Earth which is significantly different from the modern Earth. Modern Earth is layered as solid core, liquid core, solid mantle, crust, while the ancient Earth is proposed therein to be liquid core, liquid mantle, solid mantle, crust. The magnetic implications of this ancient layering have until now not been explored, likely due to the modern view of the mantle as an insulator. However the electromagnetic properties of silicate melts at lower mantle pressure and temperature conditions are widely unconstrained, and there are many factors which could contribute to high electrical conductivity in such a layer. Given the presumed young age of the inner core due to upwardly revised estimates of power requirements to drive convection in the core, and recent work alluding to potentially high electrical conductivity in magma oceans at lower mantle conditions, dynamo action during the early Earth in the hypothesized BMO is a viable alternative to the standard paradigm. The role of liquid oxides in the lower mantle contributing to magnetic field generation should be considered in concert with hypothetical core dynamo histories during the early stages of Earth's evolution. Mineral physics constraints on molten mantle conductivities will be needed to understand the coevolution of thermal and magnetic history of Earth.

[26] As our understanding of properties of mantle materials at extreme conditions improves, and should they be moderately electrically conductive, we would be afforded the good fortune of being able to test the BMO hypothesis and learn about the ancient mantle through paleomagnetic observation. The models presented here all favor an Earth protected by a magnetic shield from the earliest times, but also suggests there could have been a transitional period of reduced or absent magnetic field billions of years after Earth formation. This contrasts suggestions that there was a delayed onset of the Earth's magnetic field and would have implications for our understanding of planetary evolution.

Acknowledgments

[27] The authors thank S. Labrosse for sharing codes for thermal history models, B. Buffett for helpful discussions, and R. Jeanloz, S. Stewart, Q. Williams, D. Alfe, and S. Karato for helpful comments related to electrical conductivity. This manuscript was improved through constructive reviews by D. Gubbins and an anonymous reviewer. L. Ziegler acknowledges support from NSF-1049579, D. Stegman acknowledges support from NSF-1255040 and both authors acknowledge support from 2012 Cooperative Institute for Dynamic Earth Research (CIDER-II) workshop supported by NSF-1135452.

References

Abbott, D., L. Burgess, J. Longhi, and W. H. Smith (1994), An empirical thermal history of the Earth's upper mantle, *J. Geophys. Res.*, *99*, 13,835–13,850.

Aubert, J., D. Brito, H.-C. Nataf, P. Cardin, and J.-P. Masson (2001), A systematic experimental study of rapidly rotating spherical convection in water and liquid gallium, *Phys. Earth Planet. Int.*, *128*(1), 51–74.

Biggin, A., G. Strik, and C. Langereis (2009), The intensity of the geomagnetic field in the late-Archaean: New measurements and an analysis of the updated IAGA paleointensity database, *Earth Planets Space*, *61*, 9–22.

Buffett, B. A., H. E. Huppert, J. R. Lister, and A. W. Woods (1996), On the thermal evolution of the Earth's core, *J. Geophys. Res.*, *101*, 7989–8006.

Christensen, U. (2010), Dynamo scaling laws and applications to the planets, *Space Sci. Rev.*, *152*(1–4), 565–590.

Constable, S., and C. Constable (2004), Observing geomagnetic induction in magnetic satellite measurements and associated implications for mantle conductivity, *Geochem. Geophys. Geosyst.*, *5*, Q01006, doi:10.1029/2003GC000634.

Cuk, M., and S. Stewart (2012), Making the moon from a fast-spinning Earth: A giant impact followed by resonant despinning, *Science*, *338*, 1047–1052.

Davies, G. F. (1980), Thermal histories of convective Earth models and constraints on radiogenic heat production in the Earth, *J. Geophys. Res.*, *85*, 2517–2530.

Gaillard, F., M. Malki, G. Iacono-Marziano, M. Pichavant, and B. Scaillet (2008), Carbonatite melts and electrical conductivity in the asthenosphere, *Science*, *322*(5906), 1363–1365.

Herzberg, C., K. Condie, and J. Korenaga (2010), Thermal history of the Earth and its petrological expression, *Earth Planet. Sci. Lett.*, *292*(1), 79–88.

Hicks, D., T. Boehly, J. Eggert, J. Miller, P. Celliers, and G. Collins (2006), Dissociation of liquid silica at high pressures and temperatures, *Phys. Rev. Lett.*, *97*(2), 025502.

Holme, R. (2007), Large-scale flow in the core, in *Treatise on Geophysics*, vol. 8, edited by G. schubert, pp. 107–130, Elsevier, Amsterdam.

Karato, S. (1990), The role of hydrogen in the electrical conductivity of the upper mantle, *Nature*, *347*, 272–273.

Katsura, T. (2007), Mantle electrical conductivity, mineralogy, in *Encyclopedia of Geomagnetism and Paleomagnetism, Encyclopedia of Earth Sciences*, edited by D. Gubbins and E. Herrero-Bervera, pp. 684–688, Springer, Dordrecht.

Knittle, E., and R. Jeanloz (1986), High pressure metallization of FeO and implications for the Earth core, *Geophys. Res. Lett.*, *13*, 1541–1544.

Labrosse, S., and C. Jaupart (2007), Thermal evolution of the Earth: Secular changes and fluctuations of plate characteristics, *Earth Planet. Sci. Lett.*, *260*(3), 465–481.

Labrosse, S., J. W. Hernlund, and N. Coltice (2007), A crystallizing dense magma ocean at the base of the Earth's mantle, *Nature*, *450*(7171), 866–869.

McWilliams, R. S., D. K. Spaulding, E. J. H., P. M. Celliers, D. G. Hicks, R. F. Smith, G. W. Collins, and R. Jeanloz (2012), Phase transformations and metallization of Magnesium Oxide at high pressure and temperature, *Science*, *338*, 1330–1333.

Mosenfelder, J. L., P. D. Asimow, and T. J. Ahrens (2007), Thermodynamic properties of Mg_2SiO_4 liquid at ultra-high pressures from shock measurements to 200 GPa on forsterite and wadsleyite, *J. Geophys. Res.*, *112*, B06208, doi: 10.1029/2006JB004364.

Nagao, H., T. Iyemori, T. Higuchi, and T. Araki (2003), Lower mantle conductivity anomalies estimated from geomagnetic jerks, *J. Geophys. Res.*, *108*(B5), 2254, doi:10.1029/2002JB001786.

Ni, H., H. Keppler, and H. Behrens (2011), Electrical conductivity of hydrous basaltic melts: Implications for partial melting in the upper mantle, *Contrib. Mineral. Petrol.*, *162*, 637–650.

Ohta, K., S. Onoda, K. Hirose, R. Sinmyo, K. Shimizu, N. Sata, Y. Ohishi, and A. Yasuhara (2008), The electrical conductivity of post-perovskite in Earth's D'' layer, *Science*, *320*, 89–91.

Otsuka, K., and S. Karato (2012), Deep penetration of molten iron into the mantle caused by a morphological instability, *Nature*, *492*(7428), 243–246.

Ozima, M., K. Seki, N. Terada, Y. N. Miura, F. A. Podosek, and H. Shinagawa (2005), Terrestrial nitrogen and noble gases in lunar soils, *Nature*, *436*, 655–659.

Parker, E. (1979), *Cosmical Magnetic Fields: Their Origin and Their Activity*, Clarendon, Oxford.

Pozzo, M., C. Davies, D. Gubbins and D. Alfe (2012), Thermal and electrical conductivity of iron at Earth's core conditions, *Nature*, *485*, 355–358.

Smirnov, A., J. Tarduno, and D. Evans (2011), Evolving core conditions ca. 2 billion years ago detected by paleosecular variation, *Phys. Earth Planet. Int.*, *187*(3–4), 225–231.

Solomatov, V. (2007), Magma oceans and primordial mantle differentiation, *Treatise Geophys.*, *9*, 91–119.

Spaulding, D., R. McWilliams, R. Jeanloz, J. Eggert, P. Celliers, D. Hicks, G. Collins, and R. Smith (2012), Evidence for a phase transition in silicate melt at extreme pressure and temperature conditions, *Phys. Rev. Lett.*, *108*(6), 065701.

Stanley, S., and J. Bloxham (2006), Numerical dynamo models of Uranus' and Neptune's magnetic fields, *Icarus*, *184*(2), 556–572.

Starchenko, S., and C. Jones (2002), Typical velocities and magnetic field strengths in planetary interiors, *Icarus*, *157*(2), 426–435.

Stevenson, D. (2007), Earth formation and evolution, *Treatise Geophys.*, *9*, 1–11.

Stevenson, D. J. (2003), Planetary magnetic fields, *Earth Planet. Sci. Lett.*, *208*(1–2), 1–11.

Stixrude, L., N. de Koker, N. Sun, M. Mookherjee, and B. B. Karki (2009), Thermodynamics of silicate liquids in the deep Earth, *Earth Planet. Sci. Lett.*, *278*(3), 226–232.

Tarduno, J. A., R. D. Cottrell, M. K. Watkeys, A. Hofmann, P. V. Doubrovine, E. E. Mamajek, D. Liu, D. G. Sibeck, L. P. Neukirch, and Y. Usui (2010), Geodynamo, Solar Wind, and Magnetopause 3.4 to 3.45 Billion Years Ago, *Science*, *327*, 1238–1240.

Velimsky, J. (2010), Electrical conductivity in the lower mantle: Constraints from CHAMP satellite data by time-domain EM induction modelling, *Phys. Earth Planet. Int.*, *180*, 111–117.

Vocadlo, L. (2007), Core Viscosity, in *Encyclopedia of Geomagnetism and Paleomagnetism, Encyclopedia of Earth Sciences*, edited by D. Gubbins and E. Herrero-Bervera, pp. 104–106, Springer, Dordrecht.